Bioorganic & Medicinal Chemistry 18 (2010) 1018–1028

Contents lists available at ScienceDirect

Bioorganic & Medicinal Chemistry

journal homepage: www.elsevier.com/locate/bmc

Inhibition of monoamine oxidase by 8-benzyloxycaffeine analogues

Belinda Strydom [a], Sarel F. Malan [a], Neal Castagnoli Jr. [b], Jacobus J. Bergh [a], Jacobus P. Petzer [a,*]

[a] Pharmaceutical Chemistry, School of Pharmacy, North-West University, Private Bag X6001, Potchefstroom 2520, South Africa
[b] Department of Chemistry, Virginia Tech and Edward Via College of Osteopathic Medicine, Blacksburg, VA 24061, USA

ARTICLE INFO

Article history:
Received 30 October 2009
Revised 18 December 2009
Accepted 28 December 2009
Available online 6 January 2010

Keywords:
Monoamine oxidase
Reversible inhibition
8-Benzyloxycaffeine
Caffeine
Quantitative structure–activity relationship
Molecular docking

ABSTRACT

Based on recent reports that several (*E*)-8-styrylcaffeinyl analogues are potent reversible inhibitors of monoamine oxidase B (MAO-B), a series of 8-benzyloxycaffeinyl analogues were synthesized and evaluated as inhibitors of baboon liver MAO-B and recombinant human MAO-A and -B. The 8-benzyloxycaffeinyl analogues were found to inhibit reversibly both MAO isoforms with enzyme–inhibitor dissociation constants (K_i values) ranging from 0.14 to 1.30 μM for the inhibition of human MAO-A, and 0.023–0.59 μM for the inhibition of human MAO-B. The most potent MAO-A inhibitor was 8-(3-methylbenzyloxy)caffeine while 8-(3-bromobenzyloxy)caffeine was the most potent MAO-B inhibitor. The analogues inhibited human and baboon MAO-B with similar potencies. A quantitative structure–activity relationship (QSAR) study indicated that the MAO-B inhibition potencies of the 8-benzyloxycaffeinyl analogues are dependent on the Hansch lipophilicity (π) and Hammett electronic (σ) constants of the substituents at C-3 of the benzyloxy ring. Electron-withdrawing substituents with a high degree of lipophilicity enhance inhibition potency. These results are discussed with reference to possible binding orientations of the inhibitors within the active site cavities of MAO-A and -B.

1. Introduction

Monoamine oxidase A and B (MAO-A and -B) are flavin adenine dinucleotide (FAD) containing enzymes which catalyze the oxidation of a variety of endogenous and xenobiotic amines in the brain and peripheral tissues.[1] The two isoforms are attached to the outer mitochondrial membrane and have different substrate and inhibitor selectivities.[2] MAO-A preferentially utilizes serotonin and norepinephrine as substrates and is irreversibly inhibited by clorgyline while MAO-B preferentially utilizes benzylamine as substrate and is irreversibly inhibited by (*R*)-deprenyl. Both isoforms catalyze the oxidative deamination of dopamine.[2] Due to their roles in the metabolism of neurotransmittor amines, inhibitors of MAO-A and -B have been used in the treatment of neurological disorders. MAO-A inhibitors are used to treat depressive illness[2] while MAO-B inhibitors are useful in the treatment of Parkinson's disease (PD).[3] In the basal ganglia, oxidation by MAO-B appears to be the major metabolic pathway of dopamine and inhibitors of this enzyme may therefore slow the depletion of dopamine stores in the PD brain and posssibly elevate the concentrations of endogenous dopamine and dopamine produced from administered levodopa.[4–6] In primates, MAO-B inhibitors have been shown to enhance the elevation of dopamine concentrations in the striatum following levodopa treatment.[7] As a consequence, MAO-B inhibitors are employed as adjuvants to levodopa in the symptomatic treatment of PD.[3] MAO-B inhibitors also may exert a neuroprotective effect by reducing the formation of potentially toxic side-products associated with the metabolism of monoamines. These include H_2O_2 and aldehydes that may be neurotoxic if not rapidly metabolized to inactive compounds.[1] Since MAO-B activity as well as density increases in most brain regions with age, MAO-B inhibition may be especially relevant as a treatment strategy in the aged parkinsonian brain.[8,9]

We have reported recently that several (*E*)-8-styrylcaffeinyl analogues (**1**) (Fig. 1) are potent and reversible inhibitors of mono-

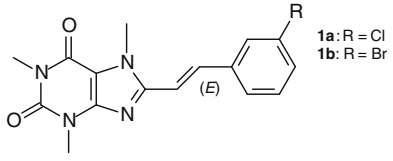

(*E*)-8-styrylcaffeinyl analogues (**1a-b**)

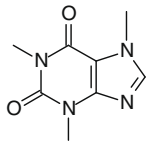

Caffeine (**2**)

Figure 1. The structures of (*E*)-8-styrylcaffeinyl analogues (**1a**–**b**) and caffeine (**2**).

* Corresponding author. Tel.: +27 18 2992206; fax: +27 18 2994243.
E-mail address: jacques.petzer@nwu.ac.za (J.P. Petzer).

0968-0896/$ - see front matter © 2010 Elsevier Ltd. All rights reserved.
doi:10.1016/j.bmc.2009.12.064

amine oxidase B (MAO-B).[10–12] The styryl side chain of these analogues is an important structural feature for inhibition since caffeine (**2**) is a weak inhibitor of MAO-B.[13] A possible explanation for this effect is that (*E*)-8-styrylcaffeinyl analogues may exhibit a dual binding mode within MAO-B with the caffeinyl ring located in the substrate cavity of the enzyme while the styryl side chain extends into the entrance cavity.[10] This would allow for more productive binding interactions with the enzyme and hence more potent inhibition. In contrast, caffeine is predicted to bind to either the substrate or entrance cavity. This view is supported by crystal structures of MAO-B that show that several potent reversible inhibitors span both active site cavities. For example, in the complex between safinamide (**3**) (Fig. 2) and MAO-B, the 3-fluorobenzyloxy side chain of safinamide is located in the entrance cavity while the propanamidyl moiety binds within the substrate cavity.[14] Similarly, the 3-chlorobenzyloxy side chain of 7-(3-chlorobenzyloxy)-4-formylcoumarin (**4**) binds in the entrance cavity of the enzyme with the coumarin ring occupying the substrate cavity.[14] Based on these observations it may be concluded that the styryl side chain of (*E*)-8-styrylcaffeinyl analogues and the benzyloxy side chains of **3** and **4** likely exhibit similar binding modes within the entrance cavity of MAO-B and are essential in stabilizing the complexes between the enzyme and the respective inhibitors. Since the styryl and benzyloxy side chains appear to have similar biological properties with respect to binding to MAO-B, a series of 8-benzyloxycaffeinyl analogues (**5a**–**g**) were synthesized and evaluated as inhibitors of baboon liver MAO-B and recombinant human MAO-B in the present study. By comparing the inhibition potencies of these analogues with those of the corresponding (*E*)-8-styrylcaffeinyl analogues, the efficacy by which the benzyloxy side chain enhances the affinity of inhibitors for the active site of MAO-B may be compared to that of styryl substitution. The 8-benzyloxycaffeinyl analogues were also evaluated as potential inhibitors of recombinant human MAO-A. Previous studies have suggested that structures with a relatively larger degree of conformational freedom may be better suited for binding to MAO-A than relatively rigid structures.[13] Since the benzyloxy side chain is relatively flexible and free to rotate about the carbon–oxygen ether bond, 8-benzyloxycaffeinyl analogues also could bind to the MAO-A active site. These studies may contribute to the discovery of a new class of potent reversible MAO inhibitors.

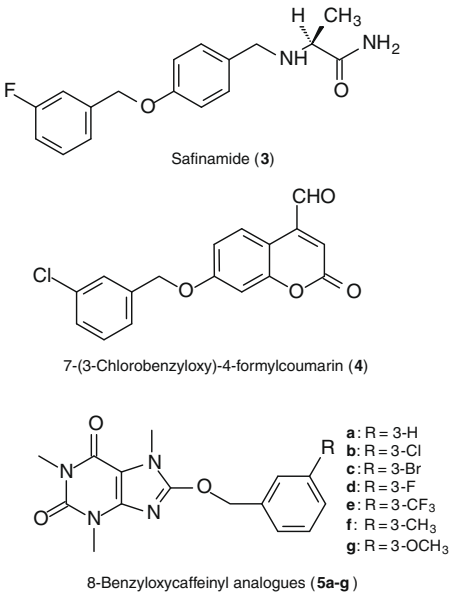

Figure 2. The structures of safinamide (**3**), 7-(3-chlorobenzyloxy)-4-formylcoumarin (**4**) and 8-benzyloxycaffeinyl analogues **5a**–**g**.

2. Results

2.1. Chemistry

The 8-benzyloxycaffeinyl analogues (**5a**–**g**) (Fig. 2) examined in this study were prepared according to a procedure previously reported for the synthesis of **5a** (Scheme 1).[15] The appropriate benzyl alcohol derivatives (**6**) were heated with dry 8-chlorocaffeine (**7**) at high temperatures (150–170 °C) in the presence of metallic sodium. The products so obtained were recrystallized from ethanol to give **5a**–**g** in low to fair yields (13–44%). 8-Chlorocaffeine, in turn, was synthesized in high yield by reacting chlorine with caffeine in chloroform.[16] The structures and purity of the target compounds were verified by mass spectrometry, ^{1}H NMR and ^{13}C NMR. For previously reported **5a**, the melting point obtained corresponded to the literature value as cited in Section 4.

2.2. General enzymology

The 8-benzyloxycaffeinyl analogues (**5a**–**g**) examined here were evaluated initially as inhibitors of baboon liver mitochondrial MAO-B and then as inhibitors of recombinant human MAO-B and MAO-A. The IC_{50} values (concentration of the inhibitor that produces 50% inhibition) for the inhibition of MAO by each test compound were determined. Since the test inhibitors exhibited a competitive mode of inhibition (see below), the IC_{50} values were converted to the corresponding K_i values (enzyme–inhibitor dissociation constants) using the Cheng–Prusoff equation.[12,17] These K_i values enabled the calculation of MAO-A/B selectivity ratios. Since a variety of caffeinyl analogues are reported to inhibit baboon liver MAO-B,[12] a comparison of the K_i values obtained with the baboon and human enzymes would make it possible to determine if the inhibition data generated with the baboon enzyme may be extrapolated to the human.

To evaluate **5a**–**g** as potential inhibitors of baboon liver mitochondrial MAO-B, the enzyme activity measurements were based on the extent to which the MAO-A/B mixed substrate, 1-methyl-4-(1-methylpyrrol-2-yl)-1,2,3,6-tetrahydropyridine (MMTP), is oxidized to the corresponding dihydropyridinium metabolite ($MMDP^+$).[18] The production of $MMDP^+$ was measured spectrophotometrically at a wavelength of 420 nm where neither the substrate (MMTP) nor the test inhibitors absorb. Inactivation of the MAO-A isoform was deemed unnecessary since baboon liver mitochondrial fractions are devoid of MAO-A activity.[18] For the purpose of converting the IC_{50} values of the test inhibitors to K_i values, a K_m value of 68.3 μM for the oxidation of MMTP by baboon liver MAO-B was used.[12]

To evaluate **5a**–**g** as potential inhibitors of recombinant human MAO-A and MAO-B, the enzyme activity measurements were based

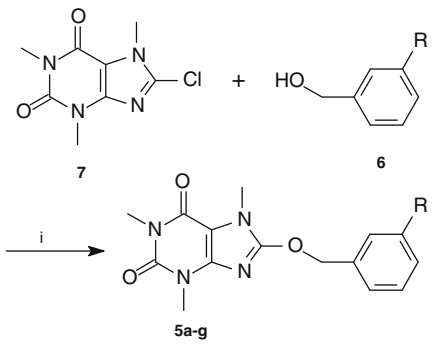

Scheme 1. Synthetic pathway to the 8-benzyloxycaffeinyl analogues **5a**–**g**. Reagent and condition: (i) Na, 170 °C.

on the extent to which kynuramine is oxidized to 4-hydroxyquinoline by the MAO isoforms.[19] The formation of 4-hydroxyquinoline was measured fluorometrically at excitation and emission wavelengths of 310 and 400 nm, respectively. None of the test inhibitors fluoresced at this excitation/emission wavelength or quenched the fluorescence of 4-hydroxyquinoline at the concentrations used for the inhibition studies. This fluorometric protocol is considerably more sensitive than the spectrophotometric method described above and was thus more suitable for the measurement of recombinant human MAO-A (0.0075 mg protein/mL) and MAO-B (0.015 mg protein/mL) activities, which were relatively low compared to the activity of baboon liver mitochondrial MAO-B (0.15 mg protein/mL) at the enzyme concentrations used for this study. For the purpose of converting the IC_{50} values of the test inhibitors to K_i values (via the Cheng–Prusoff equation),[17] K_m values for the oxidation of kynuramine by recombinant human MAO-A and MAO-B were determined (see Section 4).[12] These were found to be 16.1 ± 0.21 μM and 22.7 ± 0.72 μM for MAO-A and -B, respectively (data not shown).

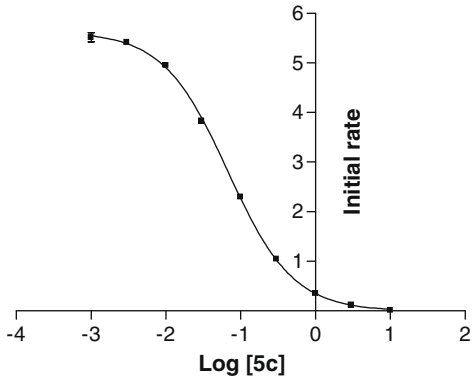

Figure 3. The sigmoidal dose–response curve of the initial rates of oxidation of kynuramine by recombinant human MAO-B vs. the logarithm of concentration of inhibitor **5c** (expressed in nM). The rates are expressed as nmoles 4-hydroxyquinoline formed/min/mg protein. The concentration kynuramine used was 30 μM, the determinations were carried out in duplicate and all values are the mean ± SD.

2.3. MAO-B inhibition studies

As shown in Table 1, all of the 8-benzyloxycaffeinyl analogues (**5a**–**g**) evaluated were found to be inhibitors of baboon liver and recombinant human MAO-B (Fig. 3). The most potent inhibitor was **5c** with an IC_{50} value of 0.068 μM for the inhibition of recombinant human MAO-B. This corresponds with a calculated K_i value of 0.023 μM (Table 2). For this series, the K_i values ranged from 0.023 to 0.59 μM, indicating that all the test compounds are relatively potent inhibitors. Since the unsubstituted homolog **5a** was the weakest inhibitor, it can be concluded that substitution at C-3 of the benzyloxy ring enhances MAO-B inhibition potency. Also, the inhibition potencies recorded with baboon and human MAO-B were found to be relatively similar. Based on this observation it can be concluded that the interactions of reversible inhibitors with human and baboon MAO-B are similar and that there are not many significant differences between the geometries and amino acid residues of the active sites of these two enzymes.

To determine the modes of inhibition, sets of Lineweaver–Burk plots were constructed for the inhibition of baboon MAO-B by one representative inhibitor, compound **5e**. As illustrated by example in Figure 4, the lines of the Lineweaver–Burk plots intersected which indicates that the mode of inhibition is competitive and that inhibition is therefore reversible. Essentially the same result was obtained when using recombinant human MAO-B as enzyme source (data not shown). These results are in accordance with expectation since (*E*)-8-styrylcaffeinyl analogues are also reported to inhibit MAO-B competitively.[10–12] To further confirm that the test inhibitors bind reversibly in the active site of MAO-B, one representative inhibitor, compound **5b**, was selected for reversibility studies. Baboon liver mitochondria were preincubated with **5b** (0.28 μM, approximately 2 × IC_{50}) for periods of 0, 15, 30, and 60 min and the rates of the MAO-B catalyzed oxidation of MMTP (50 μM) to $MMDP^+$ were measured.[20,21] As shown in Figure 5, there is no decrease of MAO-B catalytic rate with increased incubation time. Similarly, when **5b** (0.23 μM, approximately 2 × IC_{50}) was preincubated with recombinant human MAO-B for periods of 0, 15, 30, and 60 min, the rate of kynuramine (30 μM) oxidation did not decrease with increased incubation time (data not shown). From these analyses it can be concluded that **5b** interacts reversibly with the active sites of baboon and human MAO-B.

Table 1
The IC_{50} values for the inhibition of baboon liver MAO-B, human MAO-B and human MAO-A by 8-benzyloxycaffeinyl analogues **5a**–**g**

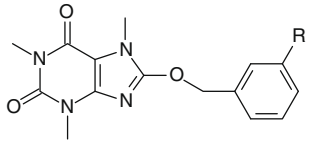

	R	IC_{50} MAO-B (baboon) μM	IC_{50} MAO-B (human) μM	IC_{50} MAO-A (human) μM
5a	H	2.49 ± 0.041	1.77 ± 0.214	1.24 ± 0.050
5b	Cl	0.120 ± 0.052	0.107 ± 0.019	0.666 ± 0.015
5c	Br	0.113 ± 0.006	0.068 ± 0.004	0.941 ± 0.009
5d	F	0.534 ± 0.091	0.542 ± 0.060	1.07 ± 0.131
5e	CF_3	0.112 ± 0.023	0.152 ± 0.004	3.72 ± 0.253
5f	CH_3	0.698 ± 0.010	0.546 ± 0.032	0.397 ± 0.018
5g	OCH_3	1.59 ± 0.609	1.01 ± 0.279	3.15 ± 0.024

All values are expressed as the mean ± SD of duplicate determinations.

Table 2
The calculated K_i values for the inhibition of baboon liver MAO-B, human MAO-B and human MAO-A by 8-benzyloxycaffeinyl analogues **5a**–**g**

	R	K_i MAO-B (baboon)[a] μM	K_i MAO-B (human)[a] μM	K_i MAO-A (human)[a] μM	SI[b]
5a	H	1.44	0.59	0.43	1.37
5b	Cl	0.069	0.036	0.23	0.16
5c	Br	0.065	0.023	0.33	0.069
5d	F	0.31	0.18	0.37	0.49
5e	CF_3	0.065	0.051	1.30	0.039
5f	CH_3	0.40	0.18	0.14	1.29
5g	OCH_3	0.92	0.34	1.10	0.31

[a] The K_i values were calculated from the experimental IC_{50} values according to the equation by Cheng and Prusoff: $K_i = IC_{50}/(1 + [S]/K_m)$ with [S] = 50 μM and K_m (MMTP) = 68.3 μM for baboon liver MAO-B. For human MAO-B, [S] = 30 μM and K_m (kynuramine) = 22.7 μM while [S] = 45 μM and K_m (kynuramine) = 16.1 μM for human MAO-A.[17]

[b] The selectivity index is the selectivity for the A isoform and is given as the ratio of K_i(MAO-B)/K_i(MAO-A).

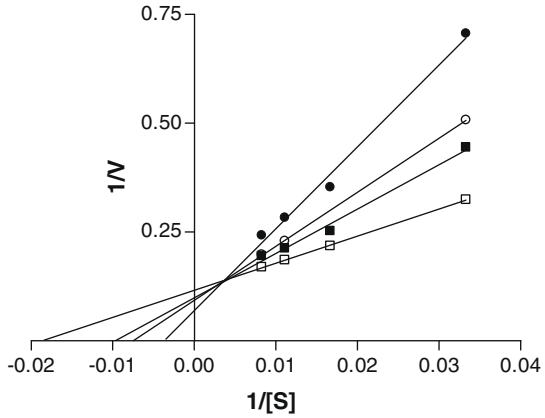

Figure 4. Lineweaver–Burk plots of the oxidation of MMTP by baboon liver MAO-B in the absence (open squares) and presence of various concentrations of **5e** (filled squares, 0.0325 μM; open circles, 0.065 μM and filled circles, 0.130 μM). The rate (*V*) is expressed as nmol product formed/min/mg protein.

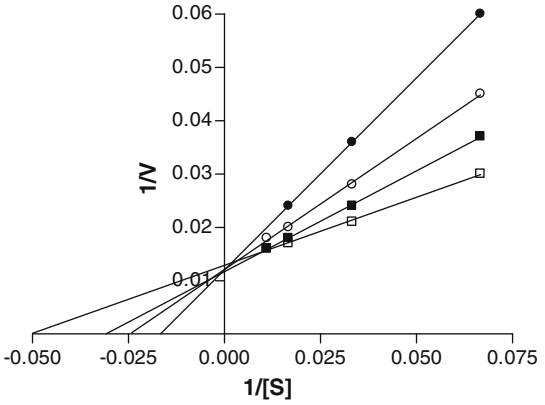

Figure 6. Lineweaver–Burk plots of the oxidation of kynuramine by recombinant human MAO-A in the absence (open squares) and presence of various concentrations of **5e** (filled squares, 0.931 μM; open circles, 1.861 μM and filled circles, 3.722 μM). The rate (*V*) is expressed as nmol product formed/min/mg protein.

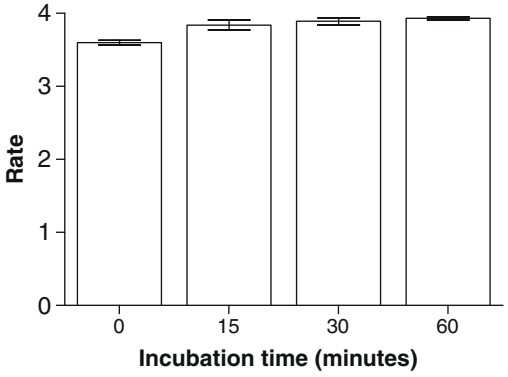

Figure 5. Time-dependant inhibition of the baboon liver mitochondrial MAO-B catalyzed oxidation of MMTP (50 μM) by **5b**. The enzyme preparation was preincubated for various periods of time (0–60 min) with **5b** (0.28 μM). The rates are expressed as nmoles $MMDP^+$ formed/min/mg protein.

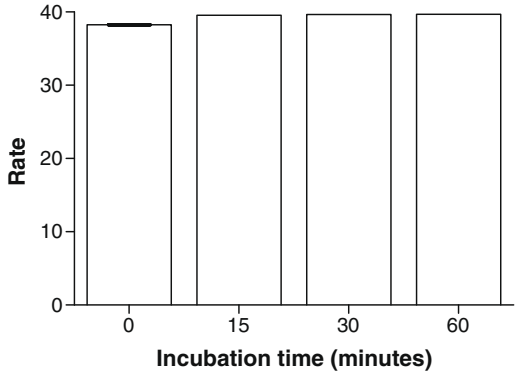

Figure 7. Time-dependant inhibition of the recombinant human MAO-A catalyzed oxidation of kynuramine (45 μM) by **5b**. The enzyme preparation was preincubated for various periods of time (0–60 min) with **5b** (1.31 μM). The rates are expressed as nmoles 4-hydroxyquinoline formed/min/mg protein.

2.4. MAO-A inhibition studies

Interestingly, the 8-benzyloxycaffeinyl analogues (**5a**–**g**) were also inhibitors of recombinant human MAO-A. The most potent inhibitor was **5f** with an IC_{50} value of 0.397 μM (Table 1) which corresponds to a calculated K_i value of 0.14 μM (Table 2). The K_i values ranged from 0.14 to 1.30 μM, indicating that **5a**–**g** are moderate to potent inhibitors of MAO-A. In general, however, these analogues were better MAO-B inhibitors. Based on the selectivity indexes (Table 2), compound **5e** displayed the highest selectivity for MAO-B (25-fold). The most potent MAO-B inhibitor of the series, **5c**, also exhibited a high degree of selectivity for MAO-B (14-fold). Compounds **5a** and **5f** were essentially nonselective.

To determine the mode of MAO-A inhibition, sets of Lineweaver–Burk plots were constructed for the inhibition of human MAO-A by compound **5e**, which was selected as a representative inhibitor. As illustrated by the example in Figure 6, the lines of the Lineweaver–Burk plots intersected which indicates that, similar to the inhibition of MAO-B, the mode of inhibition of MAO-A is competitive and reversible. The reversibility of inhibition was further demonstrated by preincubating recombinant human MAO-A with compound **5b** (1.31 μM, approximately $2 \times IC_{50}$) for periods of 0, 15, 30, and 60 min, followed by measuring the rates of MAO-A catalyzed oxidation of kynuramine (45 μM). As shown in Figure 7, MAO-A catalytic rate is not reduced with increased incubation time which indicates that **5b** binds reversibly to the active site of human MAO-A.

2.5. Quantitative structure–activity relationship (QSAR) studies

The results of the MAO-B inhibition studies (Tables 1 and 2) indicate that substitution at C-3 of the benzyloxy ring enhances MAO-B inhibition potency. To further investigate the effect of the substituents on the MAO-B inhibitory activity, a Hansch-type QSAR study was carried out. Five parameters were used to describe the physiochemical properties of the substituents. The Van der Waals volume (V_w)[22] and Taft steric parameter (E_s)[23] served as descriptors of the bulkiness of the substituents, while the lipophilicities were described by the Hansch constant (π).[23] The electronic properties were described by the classical Hammett constant (σ_m) and the Swain–Lupton constant (*F*).[23] The values of these physicochemical parameters were obtained from standard compilations.[22,23]

QSAR studies were carried out with the inhibition data obtained with baboon liver MAO-B and recombinant human MAO-B as enzyme sources and the results are summarized in Tables 3 and 4, respectively. Using the data generated with baboon liver MAO-B, a significant correlation was observed between the lipophilicity constant, π, and the inhibition potency ($\log IC_{50}$) with an R^2 value of 0.82. The statistical *F* value for this correlation was 27.8, which is higher than F_{max} value (25.32) for 95% significance.[24] A higher *F* value indicates a better fit. Improved correlations were obtained

Table 3
Correlations of the baboon liver MAO-B inhibition potencies ($\log IC_{50}$) of 8-benzyloxycaffeinyl analogues **5a**–**g** with steric, electronic and hydrophobic descriptors of the substituents at C-3 of the benzyloxy ring[a]

Parameter	Slope	*y*-Intercept	R^2	*F*	Significance[b]
σ_m	−2.25 ± 0.68	0.12 ± 0.20	0.62	10.8	0.022
F	−1.96 ± 0.89	0.18 ± 0.30	0.39	4.87	0.079
V_w	−0.49 ± 0.44	0.045 ± 0.46	0.02	1.13	0.337
π	−1.29 ± 0.24	0.19 ± 0.14	0.82	27.8	0.003
E_s	0.53 ± 0.22	0.13 ± 0.27	0.44	5.61	0.065
σ + π	−1.23 ± 0.19	0.31 ± 0.05	0.98	147	0.003
	−0.93 ± 0.10				0.0007
F + π	−1.12 ± 0.19	0.41 ± 0.064	0.98	120	0.005
	−1.07 ± 0.10				0.0004

[a] The logarithm of the IC_{50} values (expressed in μM) was used in the linear regression analysis.
[b] The significance is the fractional probability that the coefficient of the added variable is zero.

Table 4
Correlations of the recombinant human MAO-B inhibition potencies ($\log IC_{50}$) of 8-benzyloxycaffeinyl analogues **5a**–**g** with steric, electronic and hydrophobic descriptors of the substituents at C-3 of the benzyloxy ring[a]

Parameter	Slope	*y*-Intercept	R^2	*F*	Significance[b]
σ_m	−2.14 ± 0.71	0.01 ± 0.23	0.51	7.31	0.043
F	−1.97 ± 0.92	0.071 ± 0.31	0.37	4.58	0.085
V_w	−0.56 ± 0.43	0.024 ± 0.44	0.11	1.72	0.247
π	−1.27 ± 0.29	0.075 ± 0.17	0.75	18.8	0.008
E_s	0.45 ± 0.27	0.061 ± 0.32	0.23	2.83	0.153
σ + π	−1.10 ± 0.54	0.18 ± 0.14	0.84	17.3	0.112
	−0.95 ± 0.28				0.027
F + π	−1.15 ± 0.42	0.30 ± 0.14	0.89	25.4	0.052
	−1.04 ± 0.21				0.008

[a] The logarithm of the IC_{50} values (expressed in μM) was used in the linear regression analysis.
[b] The significance is the fractional probability that the coefficient of the added variable is zero.

with the addition of a second substituent parameter. A two-parameter fit with the Hammett electronic parameter (σ_m) and π versus the inhibition potency ($\log IC_{50}$) yielded the best correlation with an R^2 of 0.98 and a statistical *F* value of 147 (F_{max} = 30.18) (Fig. 8). For this correlation the probability that σ_m and π are zero is 0.3% and 0.07%, respectively. The best mathematical description

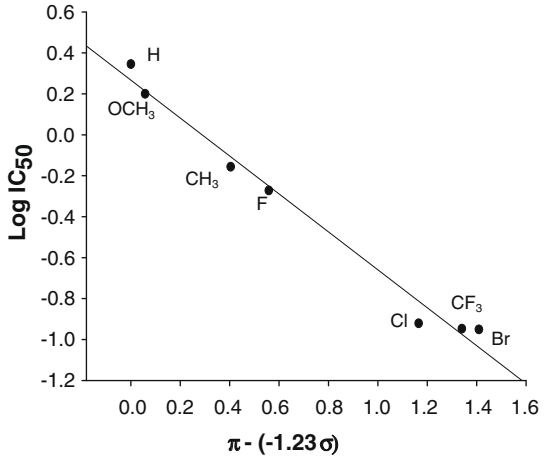

Figure 8. Correlations of the $\log IC_{50}$ values for the inhibition of baboon liver MAO-B by **5a**–**g** with the Hansch constant (π) of the substituents at C-3 of the benzyloxy ring. The π values were adjusted by the contribution of the Hammett constant (σ) as indicated on the *x*-axis title. The linear regression line is a representation of equation 1 with a correlation coefficient of 0.98.

for the binding affinity of 8-benzyloxycaffeinyl analogues (**5a**–**g**) to baboon liver MAO-B is therefore:

$$\log IC_{50} = -1.23(\pm 0.19)\sigma_m - 0.93(\pm 0.10)\pi + 0.31(\pm 0.05) \quad (R^2 = 0.98 \text{ and } F = 147) \quad (1)$$

A two-parameter fit with the Swain–Lupton constant (*F*) and π also yielded good correlations with the inhibition potency ($\log IC_{50}$) and R^2 and *F* values of 0.98 and 120 (F_{max} = 30.18), respectively, were recorded. The negative signs of the *F* (−1.12 ± 0.19) and σ_m (−1.23 ± 0.19) parameter coefficients indicate that the inhibition potencies of **5a**–**g** towards baboon liver MAO-B may be enhanced by substitution with electron withdrawing groups at C-3 of the benzyloxy ring. The negative correlations of the inhibition potencies with the π constant indicate that substituents at C-3 of the benzyloxy ring with enhanced lipophilicity may result in more potent inhibitors.

Using the inhibition data generated with recombinant human MAO-B as enzyme source, the best correlation observed was between the lipophilicity constant, π, and the inhibition potency ($\log IC_{50}$). The R^2 and statistical *F* values of this correlation were 0.75 and 18.8 (F_{max} = 25.32), respectively. A slightly improved correlation was obtained with the addition of a second substituent parameter. A two-parameter fit of *F* and π versus the inhibition potency ($\log IC_{50}$) yielded a model with an R^2 value of 0.89 and a statistical *F* value of 25.4 (F_{max} = 30.18). Similarly, a two-parameter fit of
σ_m and π versus the inhibition potency yielded a model with an R^2 value of 0.84 and a statistical *F* value of 17.3 (F_{max} = 30.18). Although these correlations are not statistically significant, the results are similar to those obtained with baboon liver MAO-B and may be viewed as further support of the notion that the interactions of reversible inhibitors with human and baboon MAO-B are similar.

A similar analysis using the inhibition data obtained with recombinant human MAO-A as enzyme source failed to yield meaningful correlations between the inhibition potencies and the substituent parameters.

2.6. Molecular modeling

In an attempt to obtain insights into the possible binding modes of the 8-benzyloxycaffeinyl analogues (**5a**–**g**) within the active sites of MAO-A and -B, molecular docking experiments were performed. The X-ray crystal structures of recombinant human MAO-A and MAO-B were obtained from the Brookhaven Protein Data Bank. The structures of MAO-A co-crystallized with harmine (PDB code: 2Z5X)[25] and MAO-B co-crystallized with safinamide (PDB code: 2V5Z)[14] were selected. These models were selected based on the relatively high resolution of the crystallographic structures and the observation that, in the complex between MAO-B and safinamide, the side chain of Ile-199 is rotated out of the normal conformation to allow for fusion of the entrance and substrate cavities. This is the preferred conformation when relatively large inhibitors, which span both the entrance and substrate cavities, bind to the active site of MAO-B.[26] In contrast, the active site of MAO-A consists of a single cavity.

For the purpose of the docking studies, the LigandFit application of the modeling software Discovery Studio 1.7[27] was used following a modification of a previously reported protocol.[13,28] The structures of **5a**–**g** were built and geometry optimized in Discovery Studio and prepared for docking with the Prepare Ligands protocol. Following the addition of hydrogen atoms and the correction of the valences of the FAD co-factors and co-crystallized ligands, the protein structures were subjected to an energy minimization while the protein backbone was constrained (see Experimental). Subse-

quently, the energy-minimized structures were deprived of the co-crystallized ligands and the backbone constraints. Following the docking procedure, the docked ligand conformations were further refined using the Smart Minimizer algorithm. Ten possible docking poses were calculated for each inhibitor. To evaluate the accuracy of this protocol, the co-crystallized ligands, harmine and safinamide, were redocked into the active sites of MAO-A and -B, respectively. The best-ranked docking solutions exhibited relatively small RMSD values from the co-crystallized ligands of 0.65 and 1.79 for harmine and safinamide, respectively. It may therefore be concluded that this protocol is suitable for docking reversible inhibitors into active site models of MAO-A and -B.

The best-ranked docking solutions obtained with the structure of MAO-B showed one prevailing pose for all of the 8-benzyloxy-caffeinyl analogues (**5a**–**g**). The inhibitors traverse both cavities of MAO-B with the caffeinyl moiety oriented towards the FAD co-factor in the substrate cavity while the benzyloxy side chain protrudes into the entrance cavity. As shown by example with inhibitor **5a**, the carbonyl oxygen at C-6 of the caffeinyl ring forms hydrogen bonds with the phenolic hydrogen of Tyr-435 (Fig. 9a). The amide functional group of the Gln-206 side chain possibly interacts with the caffeinyl ring via π–π interactions with an interplane distance of approximately 4.0 Å.[25] The benzyloxy ring is stabilized by Van der Waals interactions in the hydrophobic entrance cavity defined by Phe-103, Trp-119, Leu-164, Leu-167, Phe-168 and Ile-316.[29] Of importance is the observation that the benzyloxy ring is partly located in space that would have been occupied by the side chain of Ile-199 if it were in the normal 'closed' conformation. In the MAO-A active site the residue corresponding to Ile-199 in MAO-B is Phe-208. Since the increased size of the Phe aromatic ring compared to the side chain of Ile would prevent it from rotating into an alternative conformation, this binding mode of **5a** would not be possible in the MAO-A active site.[25,26] As shown in Figure 9b the benzyloxy ring would partially overlap with Phe-208 in the MAO-A active site.

The best-ranked docking solutions obtained with the structure of MAO-A showed that the inhibitors bind with the caffeinyl moiety oriented towards the FAD co-factor (Fig. 10a). This binding mode is similar to that observed in the MAO-B active site. As illustrated by example with compound **5a**, one hydrogen bond is observed between the carbonyl oxygen at C-2 of the caffeinyl ring and the phenolic hydrogen of Tyr-444 in the active site. Interest-

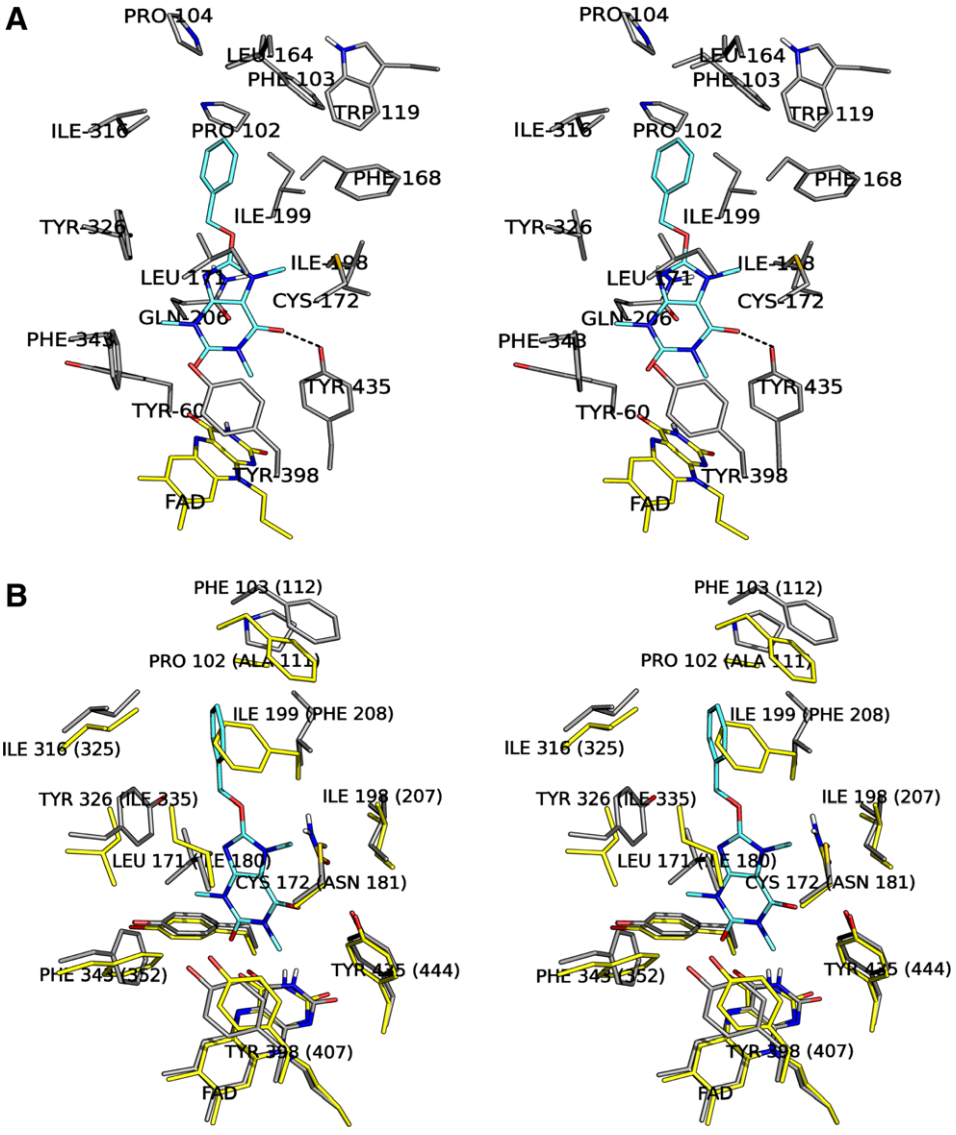

Figure 9. Stereo view representation of compound **5a** (cyan) docked within the active site of MAO-B. In panel A the active site residues (grey) of MAO-B are displayed while in panel B the active site residues of both MAO-B (grey) and MAO-A (yellow) are displayed. The FAD co-factor is shown in yellow and hydrogen bonds are indicated by the dashes. The residues are numbered based on the structure of MAO-B. The numbers given in parenthesis are the corresponding MAO-A residue identifiers.

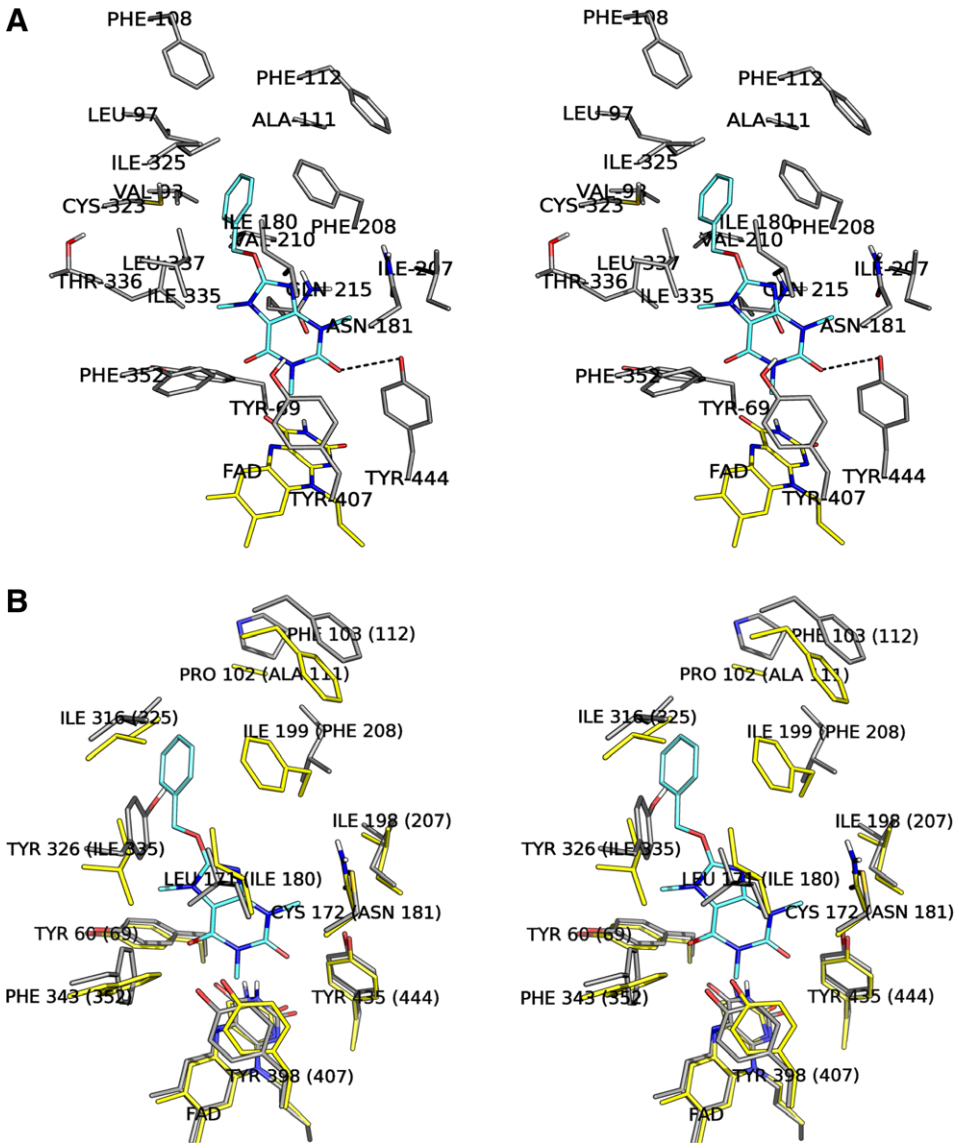

Figure 10. Stereo view representation of compound **5a** (cyan) docked within the active site of MAO-A. In panel A the active site residues (grey) of MAO-A are displayed while in panel B the active site residues of both MAO-B (grey) and MAO-A (yellow) are displayed. The FAD co-factor is shown in yellow and hydrogen bonds are indicated by the dashes. In panel B, the residues are numbered based on the structure of MAO-B. The numbers given in parenthesis are the corresponding MAO-A residue identifiers.

ingly, the caffeinyl ring is rotated through ~180° compared to the orientation in MAO-B. As expected, the benzyloxy side chains of the inhibitors are rotated to avoid unfavourable interactions with the side chain of Phe-208. For **5a**, the benzyloxy side chain is bent at the CH_2–O ether bond by about a 34° angle from the plane of the caffeinyl ring (Fig. 11). The relatively large degree of conformational freedom of the benzyloxy side chain may be an important structural feature required for MAO-A inhibition. As mentioned in Section 1, the benzyloxy side chain is relatively flexible and free to rotate about the carbon–oxygen ether bond which would enable these inhibitors to avoid structural overlap with MAO-A active site amino acid residues.[13] This bended orientation would not be possible in MAO-B since the benzyloxy ring would partially overlap with Tyr-326 in the MAO-B active site (Fig. 10b). Other interactions between the inhibitors and the enzyme include π–π interactions between the caffeinyl ring and the amide functional group of the Gln-215 side chain, with an interplane distance of approximately 3.5 Å.[25] The benzyloxy side chain may be stabilized via Van der Waals interactions with Val-210, Ile-325, Ile-335 and Leu-337.[30]

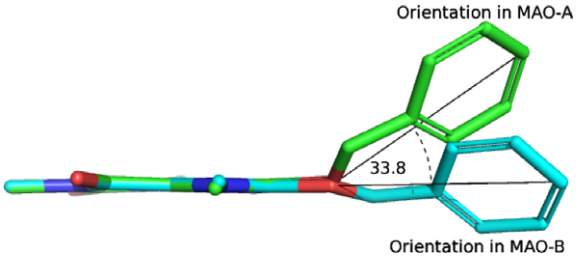

Figure 11. The docked orientations of **5a** within the active site of MAO-B (cyan) and MAO-A (green) with the caffeine rings of the two respective orientations superimposed.

3. Discussion

As mentioned in the Introduction, based on the observation that several (*E*)-8-styrylcaffeinyl analogues are potent reversible inhibitors of MAO-B,[10–12] a series of 8-benzyloxycaffeinyl analogues

(**5a**–**g**) were synthesized and evaluated as inhibitors of baboon liver MAO-B and recombinant human MAO-B. The 8-benzyloxycaffeinyl analogues were found to inhibit reversibly and potently MAO-B with K_i values ranging from 0.023 to 0.59 μM for the inhibition of the human enzyme. Similar results were obtained using baboon MAO-B as enzyme source. In general, the 8-benzyloxycaffeinyl analogues were found to be approximately equipotent to the corresponding (*E*)-8-styrylcaffeinyl analogues as inhibitors of MAO-B. For example, (*E*)-8-(3-chlorostyryl)caffeine (**1a**) (Fig. 1) has a reported IC_{50} value of 0.146 μM for the inhibition of mitochondrial baboon liver MAO-B while the corresponding 8-benzyloxycaffeinyl analogue, **5b**, inhibits baboon MAO-B with an IC_{50} value of 0.120 μM.[12] Similarly, (*E*)-8-(3-bromostyryl)caffeine (**1b**) inhibits baboon MAO-B with an IC_{50} value of 0.107 μM while the corresponding 8-benzyloxycaffeinyl analogue **5c** exhibits an IC_{50} value of 0.113 μM.[12] These results confirm that the styryl and benzyloxy side chains have similar properties with respect to binding to MAO-B and probably exhibit similar binding modes within the active site of MAO-B. The molecular docking studies suggest that the 8-benzyloxycaffeinyl analogues bind with the caffeinyl ring located within the substrate cavity of MAO-B while the benzyloxy side chain is located within the entrance cavity. (*E*)-8-Styrylcaffeinyl analogues are also thought to exhibit this dual binding mode with the styryl side chain extending towards the entrance cavity of the enzyme.[10] The proposal that the benzyloxy and styryl side chains bind within the entrance cavity of MAO-B is supported by the observation that, in the crystal structures of safinamide (**3**) and 7-(3-chlorobenzyloxy)-4-formylcoumarin (**4**) in complex with human MAO-B, the benzyloxy side chains of these inhibitors also occupy the entrance cavity of the enzyme.[14]

Interestingly, the 8-benzyloxycaffeinyl analogues were also found to be reversible inhibitors of recombinant human MAO-A with K_i values ranging from 0.14 to 1.30 μM. In general, the 8-benzyloxycaffeinyl analogues, however, displayed higher binding affinities for MAO-B than for MAO-A. The molecular docking studies indicate that the ability of the 8-benzyloxycaffeinyl analogues to bind to the MAO-A active site may, to a large degree, depend on the relatively large degree of rotation freedom of the benzyloxy side chain at the carbon–oxygen ether bond. This is in accordance with previous studies which suggested that relatively flexible inhibitors may be better accommodated in the MAO-A active site, by avoiding unfavourable interactions with active site amino acid residues.[13]

In the present study, substitution at C-3 of the benzyloxy ring has been shown to have a considerable effect on MAO-B inhibition potencies of 8-benzyloxycaffeinyl analogues. Since the benzyloxy side chain is predicted to bind within the entrance cavity of MAO-B, different interactions between the aromatic moiety, facilitated by the different C-3 substituents, and the entrance cavity residues may explain this apparent SAR. The entrance cavity of MAO-B is reported to be composed of hydrophobic amino acid residues where hydrophobic inhibitor side chains may be stabilized by Van der Waals interactions.[29] It can therefore be expected that hydrophobic substituents at C-3 of the benzyloxy ring should enhance binding affinity of the 8-benzyloxycaffeinyl analogues to MAO-B. Accordingly, the QSAR study indicates that the inhibition potencies of the test inhibitors correlate with the lipophilicity constant of the C-3 substituents, with a higher degree of lipophilicity leading to enhanced inhibition potency. These results further support the findings of the molecular docking studies which suggest that the benzyloxy side chain is bound to the entrance cavity of MAO-B. An explanation for the observed correlations between the MAO-B inhibition potency and the electronic parameters (σ_m and *F*), and thus enhancement of inhibition potency by electron withdrawing C-3 substituents, may be that electron withdrawing groups induce an electron deficiency or dipole in the benzyloxy side chain which may facilitate charge transfer or dipole interactions in the entrance cavity. The absence of correlations between the MAO-A inhibition potency and the substituent descriptor values used in the QSAR study suggest that the benzyloxy side chain of the inhibitors interact differently with MAO-A than with MAO-B. This may be the result of differing amino acid residues between the active site cavies of MAO-A and -B as well as differing binding orientations of the inhibitors in the active sites of the respective enzymes.

4. Experimental

Caution —MMTP is a structural analogue of the nigrostriatal neurotoxin, 1-methyl-4-phenyl-1,2,3,6-tetrahydropyridine (MPTP), and should be handled using disposable gloves and protective eyewear. Procedures for the safe handling of MPTP have been described previously.[31]

4.1. Chemicals and instrumentation

All starting materials not described elsewhere were obtained from Sigma–Aldrich and were used without purification. The oxalate salt of MMTP was prepared according to previously reported procedures.[32] Kynuramine.2HBr was obtained from Sigma–Aldrich. Proton (^1H) and carbon (^{13}C) NMR spectra were recorded on a Varian Gemini 300 or on a Bruker Avance III 600 spectrometer. All NMR measurements were conducted in $CDCl_3$. Chemical shifts are reported in parts per million (δ) downfield from the signal of tetramethylsilane added to the deuterated solvent. Spin multiplicities are given as s (singlet), d (doublet), t (triplet) or m (multiplet). Direct insertion electron impact ionization (EIMS) and high resolution mass spectra (HRMS) were obtained on an Autospec ETOF (Micromass) mass spectrometer. Melting points (mp) were determined on a Stuart SMP10 melting point apparatus and are uncorrected. UV–vis spectra were recorded on a Shimadzu Multispec-1501 photodiode array spectrophotometer while fluorescence spectrophotometry was conducted with a Varian Cary Eclipse fluorescence spectrophotometer. Microsomes from insect cells containing recombinant human MAO-A and -B (5 mg/mL) were obtained from Sigma–Aldrich.

4.2. Synthesis of 8-chlorocaffeine (7)

8-Chlorocaffeine was prepared according to a previously described procedure by reaction of caffeine (**2**) with chlorine in chloroform.[16] The required chlorine gas was obtained from the reaction between concentrated HCl and $KMnO_4$ and was dried by passing through concentrated H_2SO_4. High yields of 8-chlorocaffeine was obtained (94–100%) and the melting point of 188 °C corresponds to that reported in the literature (188 °C).[33] NMR data also correlated to the corresponding published values.[34]

4.3. General procedure for the synthesis of the 8-benzyloxycaffeinyl analogues (5a–g)

The 8-benzyloxycaffeinyl analogues (**5a**–**g**) were prepared according to a previously reported procedure.[15] Metallic sodium (1.76 mmol) was allowed to react with the appropriately substituted benzyl alcohol (**6**, 24.65 mmol). 8-Chlorocaffeine (**7**, 1.75 mmol) was added to the mixture and the reaction was heated at 170 °C for a period of 6 h. After the reaction was cooled, the 8-benzyloxycaffeine analogues were obtained by crystallization. In most cases the yields obtained were improved by the addition of 10–20 mL ethanol and cooling the mixture to 4 °C during the crystallization process. For previously reported **5a** the melting point was found to be 173 °C while the literature value is 172–173.5 °C.[15]

4.3.1. 8-Benzyloxycaffeine (5a)

The title compound was prepared from 8-chlorocaffeine (**7**) and benzyl alcohol in a yield of 29%: mp 173 °C, lit mp 172–173.5 °C;[15] ^{1}H NMR ($CDCl_3$) δ 3.36 (s, 3H), 3.52 (s, 3H), 3.69 (s, 3H), 5.47 (s, 2H), 7.32–7.46 (m, 5H); ^{13}C NMR ($CDCl_3$) δ 29.79 (CH_3), 29.71 (CH_3), 27.68 (CH_3), 72.52 (CH_2), 103.53 (C), 135.00 (CH), 128.84 (CH), 128.66 (CH), 128.41 (CH), 155.51 (C), 154.79 (C), 151.66 (C), 146.16 (C); EIMS *m/z* 300 ($M^{\cdot+}$); HRMS calcd 300.12224, found 300.12351.

4.3.2. 8-(3-Chlorobenzyloxy)caffeine (5b)

The title compound was prepared from 8-chlorocaffeine (**7**) and 3-chlorobenzyl alcohol in a yield of 22%: mp 174 °C; ^{1}H NMR ($CDCl_3$) δ 3.40 (s, 3H), 3.54 (s, 3H), 3.74 (s, 3H), 5.42 (s, 2H), 7.45 (s, 1H), 7.35 (m, 3H); ^{13}C NMR ($CDCl_3$) δ 29.85 (CH_3), 29.70 (CH_3), 27.69 (CH_3), 71.49 (CH_2), 103.63, 126.34, 128.44, 128.96, 129.96, 134.58, 136.96, 146.03, 151.62, 154.79, 155.17; EIMS *m/z* 334 ($M^{\cdot+}$); HRMS calcd 334.08327, found 334.08352.

4.3.3. 8-(3-Bromobenzyloxy)caffeine (5c)

The title compound was prepared from 8-chlorocaffeine (**7**) and 3-bromobenzyl alcohol in a yield of 33%: mp 169 °C; ^{1}H NMR ($CDCl_3$) δ 3.34 (s, 3H), 3.49 (s, 3H), 3.68 (s, 3H), 5.43 (s, 2H), 7.58 (s, 1H), 7.48 (d, 1H), 7.36 (d, 1H), 7.22 –7.29 (t, 1H); ^{13}C NMR ($CDCl_3$) δ 29.86 (CH_3), 29.71 (CH_3), 27.69 (CH_3), 71.43 (CH_2), 103.64, 126.85, 130.23, 131.41, 131.90, 122.66, 137.18, 146.03, 151.62, 154.79, 155.15; EIMS *m/z* 378 ($M^{\cdot+}$); HRMS calcd 380.03070, found 380.02580.

4.3.4. 8-(3-Fluorobenzyloxy)caffeine (5d)

The title compound was prepared from 8-chlorocaffeine (**7**) and 3-fluorobenzyl alcohol in a yield of 44%: mp 185 °C; ^{1}H NMR ($CDCl_3$) δ 3.35 (s, 3H), 3.5 (s, 3H), 3.69 (s, 3H), 5.43 (s, 2H), 6.98–7.08 (m, 1H), 7.11–7.22 (m, 2H), 7.30–7.38 (m, 1H); ^{13}C NMR ($CDCl_3$) δ 29.83 (CH_3), 29.69 (CH_3), 27.69 (CH_3), 71.51 (CH_2), 103.62, 115.29, 115.86, 123.74, 130.33, 137.45, 155.19, 146.05, 151.62, 161.18, 164.46; EIMS *m/z* 318 ($M^{\cdot+}$); HRMS calcd. 318.11282, found 318.11033.

4.3.5. 8-[(3-Trifluoromethyl)benzyloxy]caffeine (5e)

The title compound was prepared from 8-chlorocaffeine (**7**) and 3-(trifluoromethyl)benzyl alcohol in a yield of 22%: mp 146 °C; ^{1}H NMR ($CDCl_3$) δ 3.34 (s, 3H), 3.56 (s, 3H), 3.69 (s, 3H), 5.50 (s, 2H), 7.27–7.51 (m, 4H); ^{13}C NMR ($CDCl_3$) δ 29.85 (CH_3), 29.66 (CH_3), 27.69 (CH_3), 71.52 (CH_2), 103.67, 129.23, 131.26, 335.96, 125.65, 131.26, 122.93, 125.65, 146.01, 151.62, 154.81, 155.09; EIMS *m/z* 368 ($M^{\cdot+}$); HRMS calcd 368.10963, found 368.10714.

4.3.6. 8-(3-Methylbenzyloxy)caffeine (5f)

The title compound was prepared from 8-chlorocaffeine (**7**) and 3-methylbenzyl alcohol in a yield of 13%: mp 145 °C; ^{1}H NMR ($CDCl_3$) δ 3.42 (s, 3H), 3.58 (s, 3H), 3.74 (s, 3H), 2.43 (s, 3H), 5.49 (s, 2H), 7.24–7.34 (m, 4H); ^{13}C NMR ($CDCl_3$) δ 21.30 (CH_3), 27.64 (CH_3), 29.66 (CH_3), 29.77 (CH_3), 72.59 (CH_2), 103.47, 125.48, 128.54, 129.13, 129.56, 134.87, 138.37, 146.15, 151.63, 154.75, 155.54; EIMS *m/z* 314 ($M^{\cdot+}$); HRMS calcd 314.13789, found 314.13983.

4.3.7. 8-(3-Methoxybenzyloxy)caffeine (5g)

The title compound was prepared from 8-chlorocaffeine (**7**) and 3-methoxybenzyl alcohol in a yield of 30%: mp 144 °C; ^{1}H NMR ($CDCl_3$) δ 3.42 (s, 3H), 3.56 (s, 3H), 3.73 (s, 3H), 3.85 (s, 3H), 5.51 (s, 2H), 6.92 –7.35 (m, 4H); ^{13}C NMR ($CDCl_3$) δ 29.85 (CH_3), 29.75 (CH_3), 27.72 (CH_3), 55.27 (CH_3), 72.38 (CH_2), 103.56, 114.14, 114.07, 120.56, 129.79, 136.48, 146.16, 151.68, 154.80, 155.49, 159.80; EIMS *m/z* 330 ($M^{\cdot+}$); HRMS calcd 330.13281, found 330.13554.

4.4. Mitochondrial baboon liver MAO-B inhibition studies

Baboon liver mitochondrial fractions were isolated as described previously and stored at −70 °C.[35] Following addition of an equal volume of sodium phosphate buffer (100 mM, pH 7.4) containing glycerol (50%, w/v) to the mitochondrial isolate, the protein concentration was determined by the method of Bradford using bovine serum albumin as reference standard.[36] MMTP (K_m = 68.3 ± 1.60 μM),[12,18] served as substrate for the inhibition studies. The enzymatic reactions were conducted in sodium phosphate buffer (100 mM, pH 7.4) and contained MMTP (50 μM), the mitochondrial isolate (0.15 mg protein/mL) and various concentrations of the test inhibitors (0–100 μM). The stock solutions of the inhibitors were prepared in DMSO and were added to the incubation mixtures to yield a final DMSO concentration of 4% (v/v). DMSO concentrations higher than 4% are reported to inhibit MAO-B.[37] The final volume of the incubations was 500 μL. Following incubation at 37 °C for 10 min, the enzyme reactions were terminated by the addition of 10 μL perchloric acid (70%). The MAO-B catalyzed production of $MMDP^+$ is reported to be linear for the first 10 min of incubation under these conditions.[12] The samples were centrifuged at 16,000*g* for 10 min, and the concentrations of the MAO-B generated product, $MMDP^+$, were measured spectrophotometrically at 420 nm (ε = 25,000 M^{-1}) in the supernatant fractions.[18] The IC_{50} values were determined by plotting the initial rates of oxidation versus the logarithm of the inhibitor concentrations to obtain a sigmoidal dose–response curve. This kinetic data were fitted to the one site competition model incorporated into the Prism software package (GraphPad Software Inc.). The IC_{50} values were determined in duplicate and are expressed as mean ± standard deviation (SD). The K_i values were calculated from the experimental IC_{50} values according to the equation by Cheng and Prusoff: $K_i = IC_{50}/(1 + [S]/K_m)$ with [S] = 50 μM and K_m (MMTP) = 68.3 μM.[17]

4.5. Recombinant human MAO-A and -B inhibition studies

Microsomes from insect cells containing recombinant human MAO-A and -B (5 mg/mL) were obtained from Sigma–Aldrich, prealiquoted and stored at −70 °C. All enzymatic reactions were carried out in potassium phosphate buffer (100 mM, pH 7.4, made isotonic with KCl) containing MAO-A (0.0075 mg/mL) or MAO-B (0.015 mg/mL), various concentrations of the test inhibitor (0–100 μM) and kynuramine. The final concentrations of kynuramine in the reactions were 45 μM and 30 μM where MAO-A and -B, respectively, served as substrates. The final volume of the reactions was 500 μL. Stock solutions of the test inhibitors were prepared in DMSO and added to the reactions to yield a final concentration of 4% (v/v) DMSO. The reactions were incubated for 20 min at 37 °C and terminated with the addition of 200 μL NaOH (2 M). Distilled water (1200 μL) was added to each reaction before it was centrifuged for 10 min at 16,000*g*. The concentrations of the MAO generated 4-hydroxyquinoline in the reactions were determined by measuring the fluorescence of the supernatant at an excitation wavelength of 310 nm and an emission wavelength of 400 nm.[19] Quantitative estimations of 4-hydroxyquinoline were made by means of a linear calibration curve ranging from 0.188 to 6.25 μM. Each calibration standard was prepared to a final volume of 500 μL in potassium phosphate buffer (100 mM, pH 7.4) and contained 4% DMSO. To each standard was added 200 μL NaOH (2 M) and 1200 μL distilled water. IC_{50} values were determined by plotting the initial rate of oxidation versus the logarithm of the inhibitor concentration to obtain a sigmoidal dose–response curve. This kinetic data were fitted to the one site competition model incorporated into the Prism software package and the IC_{50} values

were determined in duplicate and are expressed as mean ± SD. The K_i values were calculated from the experimental IC_{50} values according to the equation by Cheng and Prusoff: $K_i = IC_{50}/(1 + [S]/K_m)$. For human MAO-B, [S] = 30 μM and K_m (kynuramine) = 22.7 μM while [S] = 45 μM and K_m (kynuramine) = 16.1 μM for human MAO-A.[17]

4.6. Lineweaver–Burk plots

For selected inhibitors, Lineweaver–Burk plots were constructed in order to determine the modes of inhibition. For this purpose the initial rates of oxidation at four different substrate concentrations in the absence and presence of three different concentrations of the inhibitors were used to construct Lineweaver–Burke plots. Where baboon liver mitochondrial MAO-B was used as enzyme source, compound **5e** (0.0325–0.130 μM) was selected as inhibitor and MMTP (30–120 μM) served as substrate. Where recombinant human MAO-A or -B was used as enzyme source, compound **5e** at concentrations of 0.931–3.722 μM and 0.0325–0.130 μM, respectively, was selected as inhibitor and kynuramine (15–90 μM) served as substrate. All enzymatic reactions and measurements were carried out as described above. Linear regression analysis was performed using the SigmaPlot software package (Systat Software Inc.).

4.7. Time-dependant inhibition studies

Time-dependant inhibition studies were carried out in order to determine whether a selected inhibitor, **5b**, acts as a reversible inhibitor or as a time-dependant inactivator of baboon liver MAO-B, human MAO-A and human MAO-B. The respective MAO preparations were preincubated for periods of 0, 15, 30, 60 min at 37 °C with **5b** at concentrations of 0.28 μM, 1.31 μM and 0.23 μM for baboon liver MAO-B, human MAO-A and human MAO-B, respectively.[21,28] For this purpose the concentrations of the enzyme preparations were 0.3 mg/mL baboon liver MAO-B, 0.015 mg/mL human MAO-A and 0.03 mg/mL human MAO-B. The incubations were carried out in sodium phosphate buffer (100 mM, pH 7.4) for the studies with baboon liver MAO-B and in potassium phosphate buffer (100 mM, pH 7.4, made isotonic with KCl) for studies with the recombinant human enzymes. A final concentration of 50 μM MMTP for baboon liver MAO-B, 45 μM kynuramine for human MAO-A and 30 μM kynuramine for human MAO-B were then incubated with the preincubated enzyme preparations at 37 °C for 15 min. The final volumes of these incubations were 500 μL and the final concentrations of **5b** were 0.14 μM, 0.65 μM and 0.115 μM for baboon liver MAO-B, human MAO-A and human MAO-B, respectively. These concentrations of the inhibitor are approximately equal to the IC_{50} values for the inhibition of the respective enzyme preparations by **5b**. The final concentrations of the enzyme preparations were 0.15 mg/mL baboon liver MAO-B, 0.0075 mg/mL human MAO-A and 0.015 mg/mL human MAO-B. The reactions with baboon liver MAO-B were terminated with 10 μL perchloric acid (70%) while the reactions with the recombinant human enzymes were terminated with 200 μL NaOH (2 M). A volume of 1200 μL distilled water was added to the incubations containing the recombinant human MAO preparations. The rates of formation of $MMDP^+$ and 4-hydroxyquinoline were measured as described above. All measurements were carried out in triplicate and are expressed as mean ± standard error of the mean (SEM).

4.8. K_m Determination of kynuramine for recombinant human MAO-A and -B

The steady-state oxidation rates of kynuramine by recombinant human MAO-A and -B were measured at six different substrate concentrations ranging from 2.5 μM to 80 μM. For MAO-A the final enzyme concentration in the incubations was 0.0075 mg/mL while the final concentration of MAO-B was 0.015 mg/mL. All the incubations were prepared in potassium phosphate buffer (100 mM, pH 7.4, made isotonic with KCl) and were carried out for 20 min at 37 °C. The reactions were terminated with 200 μL NaOH (2 M) and 1200 μL distilled water was added. The rates of the MAO catalyzed formation of 4-hydroxyquinoline were measured as described above. The kinetic data (initial rates as a function of substrate concentration) were fitted to a Michaelis–Menten equation using the one site binding model incorporated into the Prism software package. All measurements were carried out in duplicate and the K_m values are expressed as mean ± SEM.

4.9. QSAR studies

The values of the substituent descriptors σ_m, F, π, E_s, V_w were obtained from standard compilations.[22,23] Stepwise multiple linear regression analysis of the inhibition potencies (log IC_{50} values) as a function of the substituent descriptor values was carried out with the Statistica software package (StatSoft Inc.). In order to estimate the significance of the regression equations, the F statistic was employed. An F value higher than the critical F value (F_{max}) was judged to be significant. The F_{max} value for 95% significance for models constructed from seven log IC_{50} values (Tables 3 and 4) and which contains one descriptor (out of a possible five: σ_m, F, π, E_s, V_w) was calculated to be 25.32, while the F_{max} value for models containing two descriptors was calculated to be 30.18.[24]

4.10. Molecular docking studies

The molecular docking studies were carried out in the Windows based Discovery Studio 1.7 molecular modeling software.[27] All the inhibitors (**5a**–**g**) were constructed and the hydrogen atoms were added in Discovery Studio at pH 7. The geometries are optimized by Discovery Studio using a fast Dreiding-like forcefield (1000 iterations). Atom potential types and partial charges were subsequently automatically assigned with the Momany and Rone CHARMm forcefield and the inhibitors were prepared for docking with the Prepare Ligands protocol. The crystallographic structures of MAO-A co-crystallized with harmine (PDB code: 2Z5X)[25] and MAO-B co-crystallized with safinamide (PDB code: 2V5Z)[14] were retrieved from the Brookhaven Protein Data Bank (www.rcsb.org/pdb). Following the addition of hydrogen atoms according to the appropriate protonation states of the ionizable amino acids at pH 7, and the correction of the valences of the FAD co-factors (oxidized state) and co-crystallized ligands, the receptor models were automatically typed with the Momany and Rone CHARMm forcefield and subjected to a three step energy minimization cascade while the protein backbone was constrained. Minimisation of the receptor models were carried out since the X-ray crystal structures may contain residual energetic tensions as a result of the crystallisation process. The first step was a steepest descent minimization with the termination criteria set to a maximum of 2500 steps or a minimum value of 0.1 for the root mean square of the energy gradient. The second step was conjugate gradient minimization with the same termination criteria. The third step was an adopted basis Newton–Rapheson minimization with the termination criteria set to a maximum of 5000 steps or a minimum value for the root mean square of the energy gradient of 0.01. For this minimization cascade the implicit generalized Born solvation model with simple switching was used with the dielectric constant set to 4. The co-crystallized ligands, crystal waters and the backbone constraints were removed and the binding site was identified by a flood-filling algorithm. X-ray crystal structures of MAO-B have shown that only three active site water molecules are conserved, all in the vicinity of the FAD co-factor.[14] Preliminary docking studies in our labora-

tory suggests that caffeinyl analogues do not form hydrogen bonds with these waters, but is rather stabilized by hydrogen bond interaction between the carbonyl oxygen at C-6 of the caffeinyl ring and the phenolic hydrogen of Tyr-435. Automated docking was subsequently carried out with the LigandFit application of Discovery Studio. This docking protocol employed total ligand flexibility whereby the final ligand conformations are determined by the Monte Carlo conformation search method set to a variable number of trial runs. The docked ligands were further refined using in situ ligand minimization with the Smart Minimizer algorithm. Unless otherwise specified (see above), all the application modules within Discovery Studio were set to their default values and 10 docking solutions were allowed for each ligand.[13,28] The illustrations were generated in PyMOL.[38]

Acknowledgements

The NMR and MS spectra were recorded by André Joubert and Johan Jordaan of the SASOL Centre for Chemistry, North-West University. This work was supported by grants from the National Research Foundation and the Medical Research Council, South Africa.

Supplementary data

Supplementary data associated with this article can be found, in the online version, at doi:10.1016/j.bmc.2009.12.064.

References

1. Youdim, M. B. H.; Bakhle, Y. S. *Br. J. Pharmacol.* **2006**, *147*, S287.
2. Youdim, M. B. H.; Edmondson, D.; Tipton, K. F. *Nat. Rev. Neurosci.* **2006**, *7*, 295.
3. Fernandez, H. H.; Chen, J. J. *Pharmacotherapy* **2007**, *27*, 174S.
4. Collins, G. G. S.; Sandler, M.; Williams, E. D.; Youdim, M. B. H. *Nature* **1970**, *225*, 817.
5. Youdim, M. B. H.; Collins, G. G. S.; Sandler, M.; Bevan-Jones, A. B.; Pare, C. M.; Nicholson, W. J. *Nature* **1972**, *236*, 225.
6. Di Monte, D. A.; DeLanney, L. E.; Irwin, I.; Royland, J. E.; Chan, P.; Jakowec, M. W.; Langston, J. W. *Brain Res.* **1996**, *738*, 53.
7. Finberg, J. P.; Wang, J.; Bankiewich, K.; Harvey-White, J.; Kopin, I. J.; Goldstein, D. S. *J. Neural Transm. Suppl.* **1998**, *52*, 279.
8. Nicotra, A.; Pierucci, F.; Parvez, H.; Senatori, O. *Neurotoxicology* **2004**, *25*, 155.
9. Fowler, J. S.; Volkow, N. D.; Wang, G. J.; Logan, J.; Pappas, N.; Shea, C.; MacGregor, R. *Neurobiol. Aging* **1997**, *18*, 431.
10. Vlok, N.; Malan, S. F.; Castagnoli, N., Jr.; Bergh, J. J.; Petzer, J. P. *Bioorg. Med. Chem.* **2006**, *14*, 3512.
11. Van den Berg, D.; Zoellner, K. R.; Ogunrombi, M. O.; Malan, S. F.; Terre'Blanche, G.; Castagnoli, N., Jr.; Bergh, J. J.; Petzer, J. P. *Bioorg. Med. Chem.* **2007**, *15*, 3692.
12. Pretorius, J.; Malan, S. F.; Castagnoli, N., Jr.; Bergh, J. J.; Petzer, J. P. *Bioorg. Med. Chem.* **2008**, *16*, 8676.
13. Van der Walt, E. M.; Milczek, E. M.; Malan, S. F.; Edmondson, D. E.; Castagnoli, N., Jr.; Bergh, J. J.; Petzer, J. P. *Bioorg. Med. Chem. Lett.* **2009**, *19*, 2509.
14. Binda, C.; Wang, J.; Pisani, L.; Caccia, C.; Carotti, A.; Salvati, P.; Edmondson, D. E.; Mattevi, A. *J. Med. Chem.* **2007**, *50*, 5848.
15. Huston, R. R.; Allen, W. F. *J. Am. Chem. Soc.* **1934**, *56*, 1356.
16. Fischer, E.; Reese, L. *Justus Liebigs Ann. Chem.* **1883**, *221*, 336.
17. Cheng, Y. C.; Prusoff, W. H. *Biochem. Pharmacol.* **1973**, *22*, 3099.
18. Inoue, H.; Castagnoli, K.; Van der Schyff, C. J.; Mabic, S.; Igarashi, K.; Castagnoli, N., Jr. *J. Pharmacol. Exp. Ther.* **1999**, *291*, 856.
19. Novaroli, L.; Reist, M.; Favre, E.; Carotti, A.; Catto, M.; Carrupt, P. A. *Bioorg. Med. Chem.* **2005**, *13*, 6212.
20. Khalil, A. A.; Steyn, S.; Castagnoli, N., Jr. *Chem. Res. Toxicol.* **2000**, *13*, 31.
21. Manley-King, C. I.; Terre'Blanche, G.; Castagnoli, N., Jr.; Bergh, J. J.; Petzer, J. P. *Bioorg. Med. Chem.* **2009**, *17*, 3104.
22. Van de Waterbeemb, H.; Testa, B. In *Advances in Drug Research*; Testa, B., Ed.; Academic Press: London, 1987; pp 85–225.
23. Hansch, C.; Leo, A. *Exploring QSAR. Fundamentals and Applications in Chemistry and Biology*; American Chemical Society: Washington, DC, 1995. pp 1–124.
24. Livingstone, D. J.; Salt, D. W. *J. Med. Chem.* **2005**, *48*, 661.
25. Son, S.-Y.; Ma, J.; Kondou, Y.; Yoshimura, M.; Yamashita, E.; Tsukihara, T. *Proc. Natl. Acad. Sci. U.S.A.* **2008**, *105*, 5739.
26. Hubálek, F.; Binda, C.; Khalil, A.; Li, M.; Mattevi, A.; Castagnoli, N., Jr.; Edmondson, D. E. *J. Biol. Chem.* **2005**, *280*, 15761.
27. *Accelrys Discovery Studio 1.7*, Accelrys Software Inc., San Diego, CA, USA. 2006, http://www.accelrys.com.
28. Ogunrombi, M. O.; Malan, S. F.; Terre'Blanche, G.; Castagnoli, N., Jr.; Bergh, J. J.; Petzer, J. P. *Bioorg. Med. Chem.* **2008**, *16*, 2463.
29. Novaroli, L.; Daina, A.; Favre, E.; Bravo, J.; Carotti, A.; Leonetti, F.; Catto, M.; Carrupt, P. A.; Reist, M. *J. Med. Chem.* **2006**, *49*, 6264.
30. La Regina, G.; Silvestri, R.; Gatti, V.; Lavecchia, A.; Novellino, E.; Befani, O.; Turini, P.; Agostinelli, E. *Bioorg. Med. Chem.* **2008**, *16*, 9729.
31. Przedborski, S.; Jackson-Lewis, V.; Naini, A. B.; Jakowec, M.; Petzinger, G.; Miller, R.; Akram, M. *J. Neurochem.* **2001**, *76*, 1265.
32. Bissel, P.; Bigley, M. C.; Castagnoli, K.; Castagnoli, N., Jr. *Bioorg. Med. Chem.* **2002**, *10*, 3031.
33. Fischer, E. *Justus Liebigs Ann. Chem.* **1882**, *215*, 267.
34. Sono, M.; Toyoda, N.; Shimizu, K.; Noda, E.; Shizuri, Y.; Tori, M. *Chem. Pharm. Bull.* **1996**, *44*, 1141.
35. Salach, J. I.; Weyler, W. *Methods Enzymol.* **1987**, *142*, 627.
36. Bradford, M. M. *Anal. Biochem.* **1976**, *72*, 248.
37. Gnerre, C.; Catto, M.; Leonetti, F.; Weber, P.; Carrupt, P.-A.; Altomare, C.; Carotti, A.; Testa, B. *J. Med. Chem.* **2000**, *43*, 4747.
38. DeLano, W. L. Palo Alto, CA, USA. 2002.